Radiotherapy and Oncology 93 (2009) 331–340

Contents lists available at ScienceDirect

Radiotherapy and Oncology

journal homepage: www.thegreenjournal.com

Cervix cancer brachytherapy

# New inverse planning technology for image-guided cervical cancer brachytherapy: Description and evaluation within a clinical frame

Petra Trnková [a,*], Richard Pötter [a], Dimos Baltas [b,c], Andreas Karabis [d], Elena Fidarova [a], Johannes Dimopoulos [a], Dietmar Georg [a], Christian Kirisits [a]

[a] Department of Radiotherapy, Medical University of Vienna, Austria; [b] Department of Medical Physics & Engineering, Strahlenklinik, Klinikum Offenbach GmbH, Germany; [c] Physics Department, University of Athens, Greece; [d] Pi-Medical Ltd., Athens, Greece

ARTICLE INFO

*Article history:*
Received 14 April 2009
Accepted 24 August 2009
Available online 19 October 2009

*Keywords:*
Inverse planning
Optimisation
HIPO
Brachytherapy
Cervix

ABSTRACT

*Purpose:* To test the feasibility of a new inverse planning technology based on the Hybrid Inverse treatment Planning and Optimisation (HIPO) algorithm for image-guided cervical cancer brachytherapy in comparison to conventional manual optimisation as applied in recent clinical practice based on long-term intracavitary cervical cancer brachytherapy experience.

*Materials and methods:* The clinically applied treatment plans of 10 tandem/ring (*T*/*R*) and 10 cases with additional needles (*T*/*R* + *N*) planned with PLATO v14.3 were included. Standard loading patterns were manually optimised to reach an optimal coverage with 7 Gy per fraction to the High Risk CTV and to fulfil dose constraints for organs at risk. For each of these patients an inverse plan was retrospectively created with Oncentra GYN v0.9.14. Anatomy based automatic source activation was based on the topography of target and organs. The HIPO algorithm included individual gradient and modification restrictions for the *T*/*R* and needle dwell times to preserve the spatial high-dose distribution as known from the long-term clinical experience in the standard cervical cancer brachytherapy and with manual planning.

*Results:* HIPO could achieve a better target coverage (V100) for all *T*/*R* and 7 *T*/*R* + *N* patients. Changes in the shape of the overdose volume (V200/400) were limited. The $D_{2cc}$ per fraction for bladder, rectum and sigmoid colon was on average lower by 0.2 Gy, 0.4 Gy, 0.2 Gy, respectively, for *T*/*R* patients and 0.6 Gy, 0.3 Gy, 0.3 Gy for *T*/*R* + *N* patients (a decrease from 4.5 to 4 Gy per fraction means a total dose reduction of 5 Gy EQD2 for a 4-fraction schedule). In general the dwell times in the additional needles were lower compared to manual planning. The sparing factors were always better for HIPO plans. Additionally, in 7 *T*/*R* and 7 *T*/*R* + *N* patients all three $D_{0.1cc}$, $D_{1cc}$ and $D_{2cc}$ for vagina wall were lower and a smaller area of vagina was covered by the reference dose in HIPO plans. Overall loading times in the tandem, the ring and the needles, as well as dose distribution, were largely preserved with adaptations performed due to specific topographical variations, in particular in lateral and caudal directions.

*Conclusions:* Inverse planning based on the HIPO algorithm can produce treatment plans for cervical cancer brachytherapy which are comparable to plans based on manual optimisation as applied in clinical practice. It is essential to take into account the spatial dose distribution in addition to the DVH-based constraints. The proposed inverse planning concept is feasible for improving the therapeutic ratio and limiting substantial high-dose regions around needles.



Several new planning concepts became available as a result of the integration of 3-dimensional imaging in cervical cancer brachytherapy treatment planning. Standard loading patterns have been adapted with manual source position activation and manual dwell time adjustment. Dose and volume parameters for target structures and organs at risk (OAR) can guide this forward planning approach. In particular, the integration of magnetic resonance imaging (MRI) has allowed several centres to report dose constraint based dwell time adjustment for increased target coverage and organ sparing [1–3].

As a set of dose–volume histogram (DVH) parameters is available and certain dose limits have been established in individual centres, it is a logical step forward to think about inverse planning for cervical cancer brachytherapy. Inverse planning has already been implemented in external beam radiotherapy (EBRT) for many years [4]. Intensity-modulated radiation therapy (IMRT) enables better conformation of the high-dose region to the prescribed target volume to be achieved. The goal of optimised IMRT planning or inverse planning is to identify the beam profiles that provide optimum yield from all the physically achievable treatment plans

* Corresponding author. Address: Department of Radiotherapy, Medical University of Vienna, Währinger Gürtel 18-20, 1090 Wien, Austria.
*E-mail address:* petra.trnkova@akhwien.at (P. Trnková).

0167-8140/$ - see front matter © 2009 Elsevier Ireland Ltd. All rights reserved.
doi:10.1016/j.radonc.2009.10.004

[4]. For brachytherapy, inverse planning should result in a faster and more reproducible planning process, with better target coverage and organ sparing, especially in cases where complex topography and application techniques are involved.

Inverse planning algorithms integrate the anatomical information of each individual patient with the clinical dosimetric requirement. Dosimetric limits and dose–volume constraints are defined for each anatomical volume of interest (VOI). The task of the inverse planning algorithm is to derive adequate dwell positions and dwell time configurations that fulfil a set of limits and constraints to the highest possible degree [5–8]. The clinical dosimetric criteria for VOIs are considered by the inverse planning engines via dedicated objective functions [8]. In brachytherapy, these algorithms can also be used to calculate the optimum implant geometry, including needle positions, in a pre-plan procedure [9].

Inverse planning should reduce the overall planning work and favourably increase the therapeutic ratio. It should be user-independent and deliver cost-effective economic results. With the TPSs that handle inverse planning algorithms, the treatment planning consists of an interactive process of compromise between several objectives [6]. Several papers presenting the results of inverse planning in cervical cancer have already been published [5–7,10]. The group from the University of California, San Francisco (UCSF) stated in their work that inverse planning allows better shaping of dose distribution, is faster than conventional treatment planning and that the creation of the treatment plan can be very reproducible and safe [6,8,11]. Although inverse planning is a multi-objective problem [12–14], the common approach is the use of an aggregate objective function which takes all clinical requirements into account simultaneously [8]. Due to the multi-objective nature of the problem, there is no guarantee that all dosimetric requirements can be fulfilled. Instead, a specific trade-off between the various objectives (requirements) depending on the choice of the penalty factors [15] is delivered.

Despite the various advantages, inverse planning needs a comprehensive and "complete" set of dose and volume constraints for all target and normal tissue structures to be defined, while in manual planning several of these limitations are intrinsic due to conservative approaches which have been applied in clinical practice for a long time. These approaches shape dose distributions beginning with, and according to, standard loading patterns. For example, there are currently no dedicated dose–volume limits available for the vagina, for the CTV inside and outside the uterus (e.g. high-dose areas in the GTV of the uterus or in connective tissue, nerves, ureter and vessels), or other structures within the treated and/or irradiated volume not yet recognised as critical. However, it seems likely, that such dose–volume relationships exist. This will probably apply to both tumour control and adverse side effects. Therefore, a treatment planning approach, which takes account of the as yet unknown parameters, should be preferred. This is particularly true for inverse planning where so many degrees of freedom exist.

Manually optimised treatment planning normally leads to a typical pear-shaped isodose distribution with a unique character of the location of high-dose regions concentrated within the tumour bearing uterus and not spreading into the adjacent normal tissues. This spatial high-dose distribution has not yet been taken into account in inverse planning for cervical cancer brachytherapy. Only dose and volume constraints for a limited set of structures have been included [6–8,10]. When plan evaluation is based only on the parameters proposed by GEC-ESTRO recommendations [16,17], important changes at the high-dose level may be overlooked. At first sight, the inverse optimised plan can look better or the same as a manually optimised plan, although high-dose regions may have changed unacceptably in form and location.

The aim of this study is to introduce inverse planning into cervical cancer brachytherapy within a clinical framework, which means that the clinical experience collected over many decades in cervical cancer brachytherapy is integrated into this system [18]. A clinically valid concept for inverse planning should result in similar dose characteristics as those of the manual plans used in clinical practice [1–3,19]. For example, high-dose regions are to be directed in amount and location by integrating a control mechanism. In this specific study, a set of clinical parameters, as have been used at the Medical University of Vienna (MUV) since 1998, were chosen as the clinical framework and applied to a manual treatment planning [20,21]. These parameters have been validated within a clinical programme with a favourable therapeutic outcome for a significant patient population [22].

In order to investigate inverse planning within the framework of valid clinical settings, the new TPS Oncentra GYN v0.9.14 (Nucletron B.V., Veenendaal, The Netherlands) was used as the investigation tool. Oncentra GYN implements the Hybrid Inverse treatment Planning and Optimisation (HIPO) algorithm, originally implemented into Oncentra Prostate TPS (Nucletron B.V., Veenendaal, The Netherlands, up v3.1). HIPO is a 3D anatomy-based optimisation algorithm which is not only capable of optimising the dose distribution for a given needle and/or applicator configuration but also capable of finding an adequate needle/applicator configuration for each application. The results achieved utilizing HIPO within the proposed concept for inverse planning were compared to treatment plans based on standard manual optimisation as developed within the clinical evolution of 3D image-guided gynaecologic brachytherapy over the last decade [1–3,21].

## Methods and materials

### *Patients and treatment*

For this retrospective study 20 cervical cancer patients were randomly selected from all patients treated between June 2003 and January 2008. FIGO stage classification for local tumour stage was as follows: IB1 = 2, IIB = 17, IIIB = 1. In eight patients, the local tumour extension was 2–5 cm at the time of diagnosis and in 12 patients it was >5 cm.

All patients received 45–50.4 Gy of the whole pelvic external beam radiotherapy (EBRT) followed by brachytherapy according to the MUV protocol [1]. For the first group of 10 patients, with a mean HR CTV of 30 $cm^3$, the brachytherapy treatment was performed with a MR/CT compatible Vienna Tandem/Ring (*T*/*R*) applicator (Nucletron B.V., Veenendaal, The Netherlands) [1]. For the remaining 10 patients, with large tumours and/or unfavourable topography at the time of brachytherapy (mean HR CTV of 40 $cm^3$), a combined intracavitary/interstitial application technique, Tandem/Ring applicator and interstitial needles (*T*/*R* + *N*), was used [20,21]. The number of needles and their position in the ring were chosen according to tumour size and topography. The brachytherapy treatment schedule prescribed 7 Gy per fraction to the HR CTV. In total 4 fractions were applied in two insertions, giving 2 fractions per implant. For each patient, the plan applied for the first fraction was included into the study.

Applicator reconstruction was based on predefined applicator geometries consisting of the predefined outer shape and the related source path [23].

### *Contouring*

For all patients, GTV, HR CTV and IR CTV were prospectively contoured as target volumes, and bladder, rectum and sigmoid colon as OARs, according to the GYN GEC-ESTRO recommendations [16,17]. Additionally, a vagina wall was defined as OAR beginning in the proximal third with the fornices and going down to the distal part of the vaginal packing. In cases where the vagina wall was not clearly visible on MRI slices, it was delineated with an

estimated thickness of 4 mm. Vagina wall contour was used only for evaluation and was not included in any prospective optimisation process.

*Manual planning*

The manual treatment planning was performed in the clinical setting after MRI imaging and before irradiation of the patient based on the Vienna in-house protocol. The PLATO v14.3 TPS was used. For the *T*/*R* applicator it started with activation of the dwell positions according to a standard loading pattern [1] and with normalisation of the dose distribution to get a prescribed dose of 7 Gy per fraction in point A. The resulting dose distribution was evaluated by visual inspection of isodoses and checking the dose constraints [24].

To get the best clinically acceptable treatment plan, the loading pattern and dwell positions were subsequently adjusted as necessary. Depending on the tumour size and organ topography this optimisation continued until dose and volume constraints were fulfilled as closely as possible. A detailed description of treatment planning in a clinical practice at the MUV was published in 2005 [1].

In the case of combined intracavitary and interstitial implant, the dose distribution coming from the *T*/*R* applicator was optimised as described above. Afterwards the needles were loaded and optimised to cover the extended parts of HR CTV that were not sufficiently covered by the *T*/*R* applicator alone. The additional interstitial needles were loaded starting at the tip and stopping 1 cm from the vaginal surface. The weight of dwell positions inside the needles varied from 5% to 20% (in special cases for single positions up to 30%) of the dwell weight used for sources inside the *T*/*R* configuration to prevent high-dose regions in that part of the CTV outside the uterus. Only the dose point A, on the side where no needles were inserted, was used for normalisation to conserve the initial dose distribution of *T*/*R* alone far from the needles. If the needles were on both sides of the applicator, an alternative point, not influenced by any needle loading, was defined [21].

*Inverse planning with HIPO*

The Hybrid Inverse treatment Planning and Optimisation (HIPO) algorithm is a 3D, anatomy-based inverse optimisation algorithm developed by Karabis et al. [9]. Based on dosimetric constraints, it is able to optimise the needle placement and the dwell times. A heuristic algorithm selects needle configurations, for which the dwell times are subsequently optimised with a quasi-Newton algorithm. The objectives are linearly penalising over/under doses in target(s) while protecting OARs from overdoses [9]. HIPO is available in the Oncentra Prostate vs. 3.0 and Oncentra GYN vs. 1.0 dynamic treatment planning solutions by Nucletron B.V. HIPO supports: (a) inverse optimisation of dwell times for a given applicator/needle configuration and (b) inverse optimisation of needle positions and dwell times. In the current study only the clinically placed needles were used for inverse planning.

Furthermore, HIPO offers a function that allows optimisation of a specified part of the dwell times, given the values of the rest. The user can "lock" dwell times of selected dwell positions, i.e. fix their values so that they cannot be changed by the optimiser. This ensures freezing of the dose contribution coming from the locked dwell positions. Then HIPO can adjust the dwell times for the unlocked dwell positions in order to improve the existing dose distribution, according to the defined objectives. This feature enables a flexible implementation of different clinical scenarios, as is described in the following.

The optimisation settings consist of a maximum and/or minimum dose to a VOI and its importance factor (penalty). During this study three different optimisation settings (presets/protocols) were created (Table 1a–c). The first one (Table 1a) was used for intracavitary application alone. The other two are used for combined intracavitary and interstitial treatments. In the optimisation settings for the *T*/*R* applicator part (Table 1b), the dose to HR CTV is of low importance. When optimising the dose distribution coming from the *T*/*R* applicator, sparing of the OARs is more important. Therefore, the third optimisation set (Table 1c) serves for the optimisation of the dose coming from the needles with the aim of covering the missing parts of the HR CTV.

The proposed planning concept has two different scenarios:

*(a) Group with intracavitary T/R applicator only:*

In the first, simpler scenario, only the intracavitary applicator is used. In this case, the planning process begins with the automatic activation of the source dwell position in the *T*/*R* applicator based on the individual patient's anatomy – the so-called anatomy based loading patterns [25]: all positions, or every second dwell position, are activated within defined margins around the HR CTV and avoided within defined margins around the OARs. These margins were 20 mm for the HR CTV and 15 mm for bladder, rectum and sigmoid colon. In case of overlapping margins between target and OARs, the target had priority for source activation. The dwell positions more caudal than 1 cm above the ring level were also avoided. This loading pattern was the framework for the automatic adjustment of dwell times by the inverse optimisation.

Subsequently, inverse optimisation was applied. HIPO was asked to produce plans, using the settings given in Table 1a, which were then compared to the manual plans following the Vienna in-house protocol.

*(b) Group with combined intracavitary/interstitial applicator (T/R + N):*

In this scenario the proposed treatment planning strategy mimics the procedure of forward planning. The first part of the procedure is identical to that of the first group, but using the settings given in Table 1b. Then the following steps are taken:

- The optimised dwell times in the intracavitary applicator are locked.
- All dwell positions at the interstitial needles are activated, starting at the tip and stopping 1 cm from the vaginal surface.
- Inverse optimisation with the dedicated settings (Table 1c) is applied only for the source dwell positions within the needles.

**Table 1**
Sets of objectives – limits for OARs are coming from our constraints.

| VOI | $D_{min}$ (% PD) | Imp. factor | $D_{max}$ (% PD) | Imp. factor |
|---|---|---|---|---|
| *(a) T/R applicator alone dwell time gradient: 0.5* | | | | |
| HR CTV | 100 | 50 | 300 | 1 |
| GTV | 150 | 15 | 300 | 0.1 |
| Bladder | – | – | 88 | 10 |
| Rectum | – | – | 60 | 10 |
| Sigmoid colon | – | – | 60 | 15 |
| Normal tissue | – | – | 200 | 0.1 |
| *(b) T/R applicator (from the combined intracavitary/interstitial implant) dwell time gradient: 0.5* | | | | |
| HR CTV | 100 | 10 | 300 | 2 |
| GTV | 150 | 15 | 300 | 0.1 |
| Bladder | – | – | 88 | 20 |
| Rectum | – | – | 60 | 20 |
| Sigmoid colon | – | – | 60 | 20 |
| Normal tissue | – | – | 200 | 0.1 |
| *(c) Needles (from the combined intracavitary/interstitial implant) dwell time gradient: 0.2* | | | | |
| HR CTV | 100 | 40 | 300 | 1 |
| GTV | – | – | – | – |
| Bladder | – | – | 88 | 10 |
| Rectum | – | – | 60 | 10 |
| Sigmoid colon | – | – | 60 | 10 |
| Normal tissue | – | – | 200 | 1 |

- If the dose distribution satisfies the clinical criteria then the planning procedure stops. If not, then the dwell times in the interstitial needles are locked and previous steps are repeated until the clinical criteria are fulfilled. If this is not possible, the procedure stops when no further improvement of the plan can be achieved. In a typical case, two iterations are enough to get favourable results.

With this iterative approach it is possible to achieve an adequate coverage of HR CTV while maintaining the "typical" intracavitary dose distribution. The result of this procedure is that most of the dose contribution to the target(s) results from the source dwell positions within the intracavitary applicator while additional interstitial needles fine-tune the dose distribution. Such an approach can protect the uterus and its surrounding region from high doses.

HIPO provides a number of functions that facilitate following the clinical experience as developed in a specific clinical setting. Among them is the ability to handle multiple targets simultaneously, the dedicated objective for the normal tissue and the dwell time gradient restriction. In addition HIPO enables intersections of each target volume with other targets, or even with OARs, to be defined and such intersections in the optimisation process to be considered. These targets can be in turn boost volumes.

The dedicated normal tissue objective allows the user to put a dose limit and a penalty for the tissue that was not delineated as any specific VOI, so minimizing the dose to this tissue. The dwell time gradient restriction is an extra constraint which controls the smoothness of the dwell times along any part of the implant (Table 1). It avoids large time differences between neighbouring dwell positions and therefore also avoids the presence of isolated positions with high dwell times which can result in hot spots.

### *Dose and volume constraints*

In order to reach total biologically weighted doses, a D90 of 85 $Gy_{\alpha\beta 10}$ for the HR CTV, a $D_{2cc} < 90\ Gy_{\alpha\beta 3}$ for bladder, and a $D_{2cc} < 70\ Gy_{\alpha\beta 3}$ for rectum and sigmoid colon, the physical dose constraints per fraction were D90 > 7 Gy (HR CTV), $D_{2cc} \leqslant 6.2$ Gy (bladder) and $D_{2cc} \leqslant 4.4$ Gy (rectum, sigmoid colon) for our treatment schedule [24]. The HR CTV coverage had to be always at least 90%.

### *Evaluation*

The evaluation was based on the dosimetric parameters proposed by GYN GEC ESTRO [17]. In addition, the following parameters that reflect the spatial distribution of high-dose regions were considered in the evaluation:

- Absolute volume of normal tissue receiving a certain reference dose (absolute volume of reference dose with the exclusion of absolute volumes of HR CTV and the applicator volume outside the HR CTV receiving a reference dose). The reference doses were defined as 7 Gy (PD), 14 Gy (2 × PD) and 28 Gy (4 × PD) per fraction. That means the volumes V100, V200 and V400, respectively, were checked. The part of the applicator inside of the HR CTV (~0.5–1.5 $cm^3$) was included in the HR CTV to be consistent with current practice in most centres [17].
- Total sum of dwell times within the tandem, ring and all needles.
- Dosimetric evaluation of vagina wall as an OAR most close to the applicator.
- Sparing factors defined as $D_{2cc}$ for a certain OAR divided by D90 of the HR CTV.

The statistical significance of the results was proven with a two-sided paired *t*-test with level of significance at 0.05.

## Results

### *Dosimetric evaluation and sparing factors*

An example of the dose distribution resulting from the manual optimisation and from the inverse optimisation with the HIPO algorithm is presented in Fig. 1. The mean values and standard deviations of the dosimetric parameters together with the sparing factors and the statistical significance of all evaluated parameters for both HIPO and manual plans are presented in Table 2. The intracavitary and combined intracavitary/interstitial implants were analysed separately.

For the first group of patients with *T*/*R* applicator alone, HIPO resulted in treatment plans with higher average values for V100, D90 and D100 for GTV and HR CTV and D90 and D100 for IR CTV, whereas the mean $D_{2cc}$ for bladder, rectum, and sigmoid colon were lower in comparison to manual optimisation. Only the differences in V100 ($p = 0.006$) and D90 ($p = 0.011$) for the HR CTV and $D_{2cc}$ for the rectum ($p < 0.001$) were statistically significant. The results in the form of bar graphs are presented in Fig. 2a. The V100 for the HR CTV was always higher, or equal (in case of 100% coverage) for all HIPO plans. In seven cases the D90 was higher, while in three cases with D90 values above 8 Gy, the inverse optimisation resulted in a decrease (from 8.3 to 8.1 Gy, from 8.1 to 8.0 Gy, and from 10.8 to 9.9 Gy). HIPO resulted in a higher $D_{2cc}$ for the bladder (up to 0.5 Gy) in three cases, but never above the dose limit of 6.2 Gy. For the rectum, $D_{2cc}$ was always lower and for sigmoid colon three HIPO plans resulted in higher dose values but never more than 0.2 Gy. The rectum and sigmoid colon $D_{2cc}$ of lower than or equal to 4.4 Gy were reached for all HIPO cases.

Similar results were obtained for the second group of patients treated with the combined intracavitary/interstitial implant. The results in the form of bar graph are presented in Fig. 2b. The difference in the IR CTV parameters was not statistically significant. Concerning the HR CTV parameters, three HIPO plans had lower V100 of up to −1.4%; four had lower D90 of up to −0.4 Gy. These four HIPO plans resulted in a D90 of 7.5, 9.7, 8.0 and 8.7 Gy. In two cases the bladder $D_{2cc}$ was higher, but not reaching more than 5.8 Gy. The same two cases were the only ones with increased rectum doses, but again not reaching more than 4.3 and 3.6 Gy, respectively. No case with higher sigmoid colon doses was observed ($p = 0.016$).

The sparing factor was always better for HIPO cases, as presented in Table 2. For all three OARs in the cases with the *T*/*R* configuration and for bladder and sigmoid colon in *T*/*R* + *N* the difference was statistically significant. The total volumes of the prescribed dose (7 Gy) and twice the prescribed dose (14 Gy) were very similar between both optimisation methods, with smaller average values for the HIPO plans. Both parameters were significant in the case of *T*/*R* + *N* configuration (Table 2).

### *Absolute volume of normal tissue receiving a reference dose*

The results of absolute volumes of the *T*/*R* and combined *T*/*R* + *N* applicators are presented in Table 3. The mean volumes receiving reference doses were smaller in the treatment plans calculated with HIPO. However, only the difference in the V100 parameter for *T*/*R* configuration was statistically significant ($p = 0.036$).

### *Loading times*

The absolute loading times for both types of implant are listed in Table 4. All the times were normalised to a source strength of 40,820 cGy $cm^2$ $h^{-1}$ to account for the source decay. The mean total treatment time was lower for HIPO plans. The ratio of loading times between the tandem and the ring was changed. HIPO re-

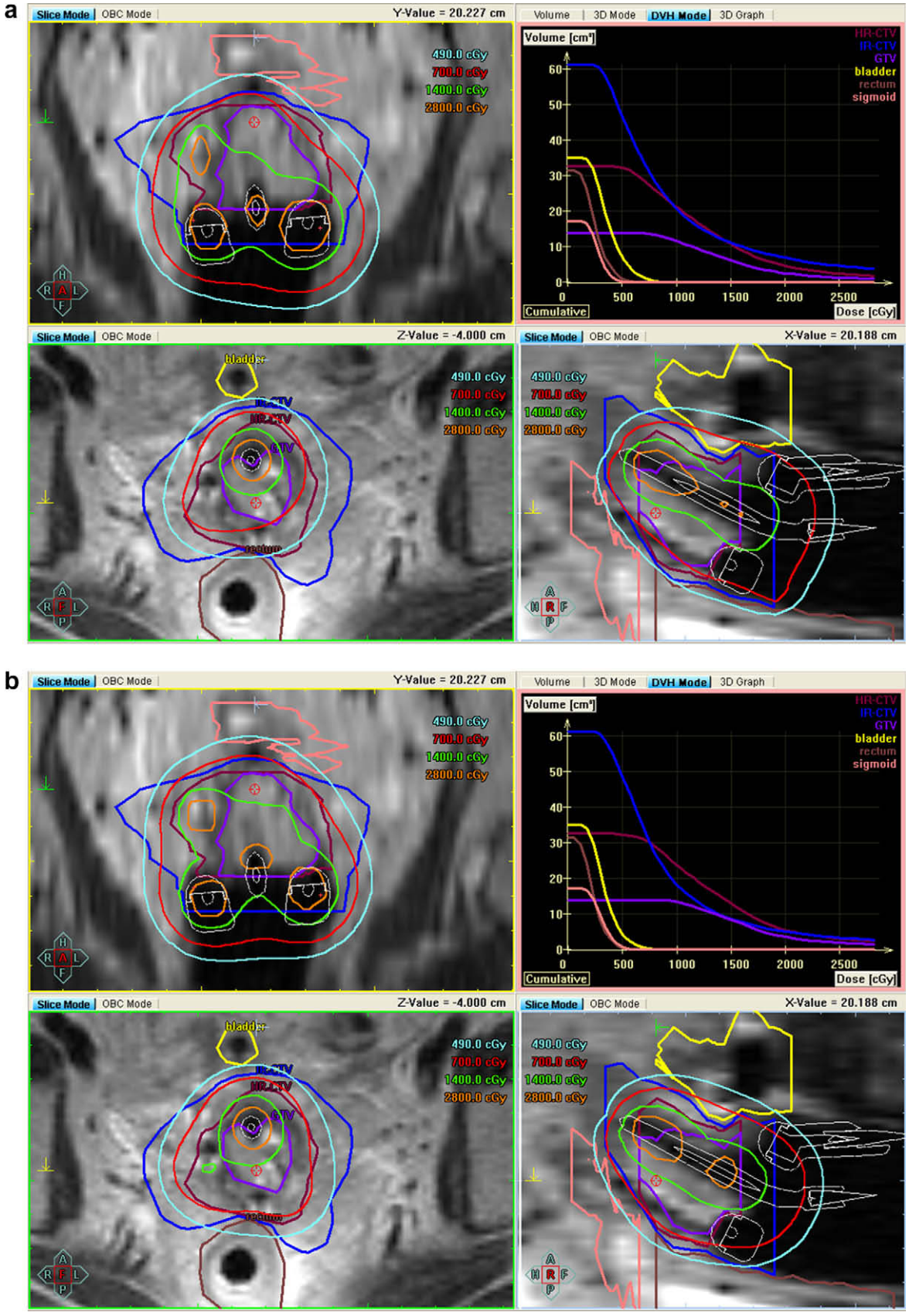


**Fig. 1.** Comparison of the dose distribution between the manually optimised treatment plan (a) and the treatment plan optimised with the HIPO algorithm (b). The displayed views are coronal, DVH, transversal and sagittal (from left to right, from up down).

**Table 2**
Dosimetric comparison between manual plan and HIPO plan for a single fraction; all doses are physical doses. Sparing factor is defined as $D_{2cc}$ for a certain OAR divided by D90 of HR CTV.

| | *T/R* | | | *T/R + N* | | |
|---|---|---|---|---|---|---|
| | Manual | HIPO | *p* | Manual | HIPO | *p* |
| HR CTV: V100 (%) | 95.8 ± 3.5 | 97.9 ± 2.3 | **0.006** | 94.7 ± 3.3 | 95.7 ± 2.5 | 0.123 |
| HR CTV: D90 (Gy) | 8.2 ± 1.1 | 8.6 ± 0.9 | 0.138 | 8.0 ± 0.9 | 8.1 ± 0.7 | 0.429 |
| HR CTV: D100 (Gy) | 5.2 ± 1.0 | 5.8 ± 0.7 | **0.011** | 4.7 ± 1.0 | 4.8 ± 1.0 | 0.714 |
| GTV: V100 (%) | 99.8 ± 0.6 | 100 ± 0.0 | 0.279 | 99.2 ± 1.7 | 99.9 ± 0.3 | 0.183 |
| GTV: D90 (Gy) | 12.6 ± 3.0 | 13.5 ± 2.2 | 0.164 | 10.8 ± 1.7 | 11.7 ± 1.3 | 0.064 |
| GTV: D100 (Gy) | 8.8 ± 2.5 | 9.6 ± 2.0 | 0.062 | 7.1 ± 1.6 | 8.2 ± 1.6 | **<0.001** |
| IR CTV: D90 (Gy) | 4.2 ± 0.4 | 5.2 ± 0.2 | 0.083 | 5.3 ± 0.6 | 5.1 ± 0.5 | 0.112 |
| IR CTV: D100 (Gy) | 1.8 ± 0.6 | 2.8 ± 0.2 | 0.162 | 2.7 ± 0.5 | 2.6 ± 0.5 | 0.745 |
| Bladder: $D_{2cc}$ (Gy) | 5.2 ± 0.9 | 5.0 ± 1.2 | 0.248 | 5.4 ± 0.5 | 4.8 ± 0.8 | **0.018** |
| Rectum: $D_{2cc}$ (Gy) | 3.5 ± 1.0 | 3.1 ± 0.8 | **<0.001** | 3.7 ± 0.7 | 3.4 ± 0.8 | 0.085 |
| Sigmoid c.: $D_{2cc}$ (Gy) | 4.2 ± 0.4 | 4.0 ± 0.5 | 0.059 | 4.2 ± 0.9 | 3.9 ± 1.0 | **0.016** |
| Implant: $V_{PD}$ ($cm^3$) | 81.1 ± 16.0 | 76.3 ± 19.4 | 0.284 | 95.4 ± 13.6 | 81.1 ± 23.4 | **0.003** |
| Implant: $V_{2xPD}$ ($cm^3$) | 25.4 ± 5.1 | 24.1 ± 6.0 | 0.180 | 31.2 ± 4.2 | 25.3 ± 6.7 | **<0.001** |
| Bladder: Sparing f. | 0.64 ± 0.13 | 0.59 ± 0.15 | **0.009** | 0.69 ± 0.11 | 0.60 ± 0.11 | **0.009** |
| Rectum: Sparing f. | 0.44 ± 0.14 | 0.37 ± 0.10 | **0.005** | 0.48 ± 0.10 | 0.42 ± 0.10 | 0.071 |
| Sigmoid c.: Sparing f. | 0.52 ± 0.09 | 0.47 ± 0.08 | **0.010** | 0.54 ± 0.14 | 0.49 ± 0.14 | **0.005** |

Note: bold values indicate $p \leqslant 0.05$.

duced the loading of the ring and increased the loading of the tandem. However, only the difference between the loading time in the ring in the *T/R* application was statistically significant ($p = 0.035$).

The mean sum of the loading times over all needles was significantly lower in HIPO plans ($p = 0.037$), as well as the mean maximum needle loading time referring to one needle with the highest sum of dwell times over all dwell positions compared to other needles loaded in a given patient ($p = 0.045$).

### *Vagina wall*

Results for the volume of vagina receiving prescribed dose, two and four times prescribed dose and for $D_{2cc}$, $D_{1cc}$ and $D_{0.1cc}$ are presented in Table 5. For this group of patients, HIPO can lead to better sparing of the vagina wall in terms of lower dose received and smaller area covered by the reference dose. However, the results were significant only for $D_{0.1cc}$ in *T/R* implants and for V200 and $D_{1cc}$ in *T/R + N*.

## Discussion

The department of radiotherapy at MUV has a tradition of image-based manual optimisation dating back to the early 90s which has shown promising results for local control and side effects [22,26]. For more than a decade, cervical cancer patients have been treated with a dedicated manual treatment planning concept [1,21,27]. The treatment plans are characterised by pear-shaped isodose distribution with a loading pattern that is generally not substantially different from the standard loading pattern, while the high-dose regions show a specific location mainly limited to the region around the intrauterine tandem and the vaginal sources. Loading and dwell times were changed to reach the minimum dose constraints for the target and maximum dose requirements for the OAR, but not necessarily to achieve the highest possible conformity, in particular for small tumours and small HR CTVs.

### *Inverse planning*

For reasons of making the treatment planning process more automatic and reproducible, inverse optimisation can be integrated into the treatment planning process. One of the inverse planning algorithms, IPSA, was published by the UCSF group [5,6,10]. It is based on the simulated annealing and inverse optimizer and takes all parts of the applicator into account at the same time and with the same weighting. Such an optimisation is problematic in controlling the location of the high-dose regions [5] because the same amount of the dose as that from the *T/R* applicator can be delivered from the additional needles. The work of Chajon et al. [5] describes the need for the supplementary tools to consider more parameters than just those introduced by the GYN GEC-ESTRO recommendations [17]. The authors proposed defining help structures around the applicator to force the optimiser engine to find more homogenous dwell time distributions, and to prevent unwanted hot spots within the treated volume. However, the creation of a lot of help structures can be time consuming and therefore not effective.

An alternative concept was presented in this paper. It is fundamentally different from what has been presented so far. The HIPO algorithm was not only integrated into the treatment planning system but it was also fine-tuned in order to fulfil the criteria of the MUV requests on the dose distribution. It represents a feasible solution for controlling hot spot regions in general, and more specifically, for avoiding hot spots in normal tissue, either by a single run in the case of the *T/R* applicator (first group of patients) or integrated in an iterative procedure (second group of patients). Its features, like the anatomy based loading patterns and the dwell time gradient restriction, have the potential to support the pear-shaped dose distribution. This is especially the case for the inverse optimisation tool that allows working on a restricted part of the implant, taking into consideration the dose contribution of the remaining part and keeping this constant. Making use of this feature, it is possible, for example, to keep an adequately optimised dose distribution result from the *T/R* applicator and to fine-tune the dose at the lateral extension of the underdosed parts of the target volume, utilizing only the additionally inserted interstitial needles at that place.

### *Dosimetric analysis*

Analysis of the dosimetric evaluation parameters in Table 2 as recommended and used by the international community for evaluation [1–3,16,17] shows that HIPO is able to produce clinically acceptable plans in terms of the DVH parameters. In Fig. 2 all dosimetric parameters are presented together. In general, the use of HIPO resulted in better parameters for the target structures and the OARs than the manual optimisation, but the difference failed statistical significance. However, it is important to emphasize that plan ranking is not based on a single DVH parameter. In our case, just the higher V100 and/or D90 were not enough to decide whether the inverse plan was better or not. The simultaneous improvement in the target volumes constraints and the OARs con-

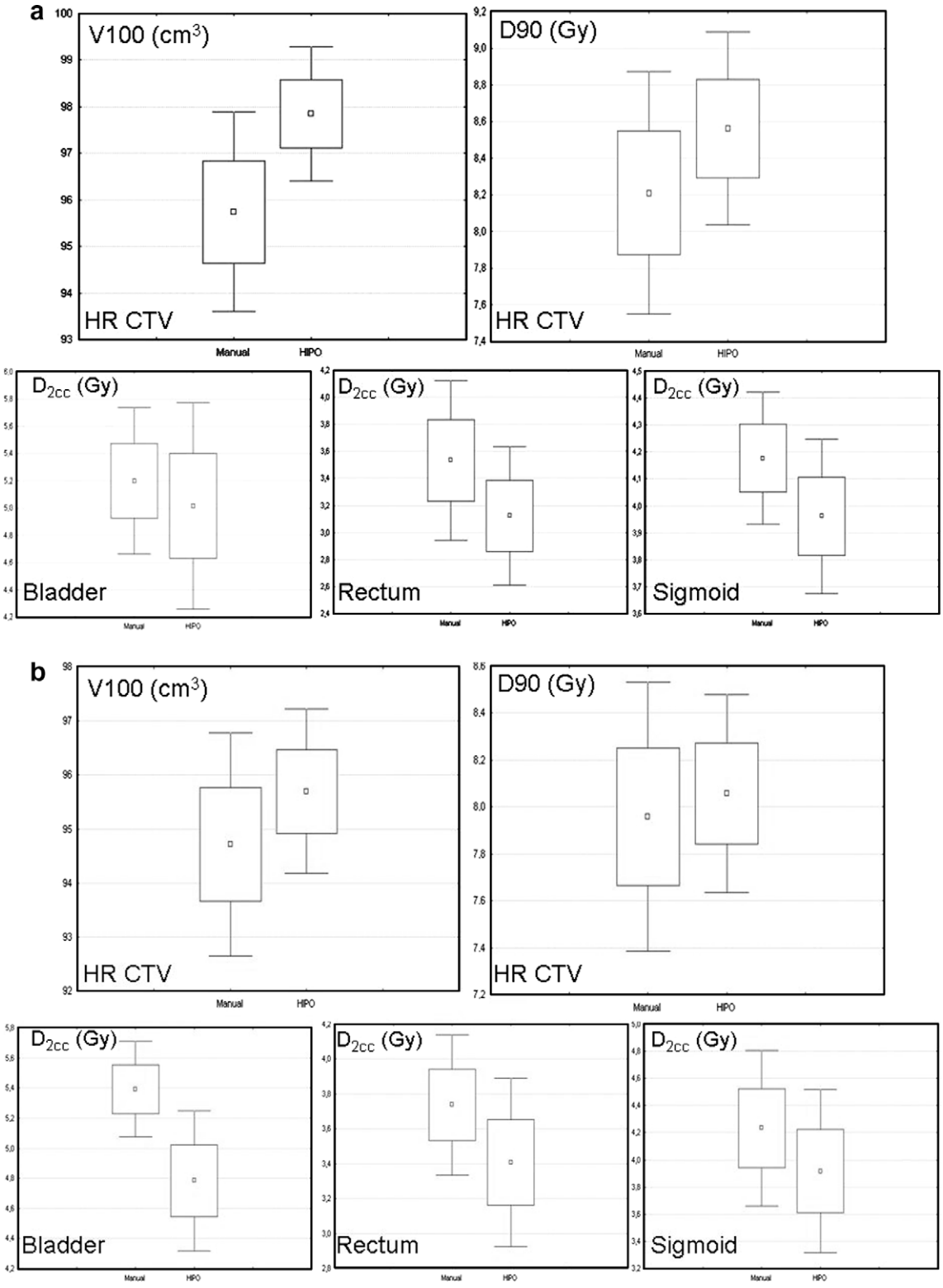


**Fig. 2.** Comparison of the main dosimetric parameters (D90 and V100 for HR CTV, $D_{2cc}$ for bladder, rectum and sigmoid) used for treatment plan evaluation in form of bar graphs. (a) Tandem/ring and (b) tandem/ring + interstitial needles.

straints was crucial. This characteristic is reflected in the therapeutic ratio, i.e. sparing factors. The sparing factors were significantly better for all OARs (except for the rectum in the $T/R + N$ configuration with $p = 0.08$) in the case of plans optimised by HIPO. This means that the presented concept for inverse optimisation could also result in a target dose decrease if the target related parameters still fulfilled the prescription, but the dose to OARs can be decreased below their upper limits. This is particularly challenging in a daily clinical routine, with limited time available for the interactive forward approach. A clear benefit of inverse planning is that all parameters and their respective predefined lower and upper limits are taken into account in parallel.

**Table 3**
Absolute volume of normal tissue receiving reference dose for *T/R* and *T/R + N* applicator (mean ± standard deviation): this volume was defined as whole implant volume without HR CTV and applicator volumes.

| | *T/R* | | | *T/R + N* | | |
|---|---|---|---|---|---|---|
| | Manual | HIPO | *p* | Manual | HIPO | *p* |
| V100 ($cm^3$) | 31.4 ± 10.5 | 29.2 ± 10.9 | 0.587 | 35.7 ± 9.3 | 28.8 ± 12.4 | **0.036** |
| V200 ($cm^3$) | 3.9 ± 2.3 | 3.5 ± 2.1 | 0.648 | 4.0 ± 1.7 | 2.7 ± 2.3 | 0.115 |
| V400 ($cm^3$) | 0.5 ± 0.6 | 0.1 ± 0.6 | 0.185 | 0.5 ± 0.4 | 0.6 ± 0.8 | 0.599 |

Note: bold values indicate $p \leqslant 0.05$.

**Table 4**
Absolute loading times of tandem, ring and additional needles for *T/R* patients (a) and *T/R + N* (b); these times are sums over all dwell positions in a certain part of the implant. Regarding the needles, it is the sum over all dwell positions in all needles together. Maximum needle loading time refers to one needle in which the sum of all dwell positions was highest compared to other needles loaded in a given patient.

| | Manual | HIPO | *p* |
|---|---|---|---|
| *(a) T/R* | | | |
| **Total treatment time (s)** | **374 ± 49** | **357 ± 63** | 0.241 |
| Ring (s) | 206 ± 48 | 166 ± 43 | **0.035** |
| Tandem (s) | 168 ± 52 | 191 ± 58 | 0.164 |
| *(b) T/R + N* | | | |
| **Total treatment time (s)** | **403 ± 38** | **351 ± 92** | 0.056 |
| Ring (s) | 199 ± 20 | 151 ± 79 | 0.105 |
| Tandem (s) | 144 ± 25 | 170 ± 59 | 0.261 |
| Σneedles (s) | 60 ± 37 | 31 ± 18 | **0.037** |
| Max needle (s) | 32 ± 17 | 19 ± 10 | **0.045** |

Note: bold values indicate $p \leqslant 0.05$.

**Table 5**
Dosimetric evaluation of vagina wall.

| | *T/R* | | | *T/R + N* | | |
|---|---|---|---|---|---|---|
| | Manual | HIPO | *p* | Manual | HIPO | *p* |
| V100 ($cm^3$) | 3.1 ± 1.2 | 2.8 ± 1.6 | 0.362 | 3.5 ± 0.8 | 2.5 ± 1.4 | 0.079 |
| V200 ($cm^3$) | 0.8 ± 0.5 | 0.5 ± 0.5 | 0.109 | 0.8 ± 0.3 | 0.4 ± 0.4 | **0.045** |
| V400 ($cm^3$) | 0.0 ± 0.0 | 0.0 ± 0.0 | 0.112 | 0.0 ± 0.1 | 0.0 ± 0.0 | 0.211 |
| $D_{2cc}$ (Gy) | 9.1 ± 2.2 | 8.3 ± 2.3 | 0.150 | 9.7 ± 1.5 | 7.8 ± 2.3 | 0.055 |
| $D_{1cc}$ (Gy) | 12.3 ± 3.0 | 10.9 ± 3.0 | 0.146 | 15.3 ± 7.3 | 10.2 ± 2.9 | **0.039** |
| $D_{0.1cc}$ (Gy) | 21.1 ± 4.2 | 17.5 ± 4.6 | **0.029** | 20.4 ± 4.0 | 17.5 ± 7.2 | 0.328 |

Note: bold values indicate $p \leqslant 0.05$.

The use of upper limits for the target dose has not yet been introduced in the Vienna clinical setting. In some cases, in particular with small tumour volumes and favourable situation of the OARs, the total dose for the D90 therefore results in more than 100 Gy. For such cases it might be appropriate to consider the use of a higher importance factor for an upper level of D90 in order to limit the dose inhomogeneity within the target.

Inverse planning can lead to underdosing of the target volumes that are not delineated such as cranially in the case of flat HR CTV with only lateral extensions. Therefore, the resulting dose after inverse optimisation should not be that conformal. For this reason specific tools were introduced into the optimisation process with HIPO. These tools will be discussed later. Moreover, additional target structures can be delineated, e.g. IR CTV, LR CTV (low-risk CTV) and lower constraints for these volumes can be defined. However, in the current study, no constraints for the IR CTV were used and no significant differences in the DVH in these volumes were observed.

### *Pear-shaped dose distribution and high-dose regions*

A major shortcoming of the literature published so far [5,6] is the presentation of dosimetric parameters as such without relation to tumour, cervix or normal tissue topography. The parameters reported do not show the location of high-dose regions within and/or outside the tumour or the target. The dose to the vagina and any other anatomical structures of interest like ureter, nerves, vessels, connective tissue in the parametrium is not given because these structures cannot currently be contoured. However, they are of clinical interest from a mid- or long-term perspective. It may well happen that high doses include some structures outside the uterus when using inverse planning algorithms. This may have clinical implications which we are not aware of at present. In our opinion, it is therefore clinically more appropriate to take these non-defined anatomical structures into consideration by adhering to the typical pear-shaped isodose form and not allowing for major deviations, particularly in high-dose regions for the tumour, target and even for these non-defined anatomical structures at risk. This framework has been used with great success for many decades, in regard to both disease control and reducing adverse side effects [22,28,29]. An entire change of this dose distribution is possible, for example with IPSA [6–8,10], but should therefore be discussed very critically, as there does not seem to be a clinical need for this. The clinical use of the IPSA concept should be handled with extreme caution or the concept should be adapted as proposed by Chajon [5]. The evolution of inverse treatment planning concepts should be driven by the provision of comprehensive clinical evidence. As more clinical data on these not defined anatomical structures will be gathered in the future, we will be able to further direct our treatment planning concept towards an even more tailored approach.

There is one other major issue regarding this advanced treatment planning as well as the manual planning approach: why keep the pear-shaped isodose distribution and not replace it by a highly conformal dose distribution around the HR CTV even when the dose constraints for OARs are not violated? This would imply that the target concept as introduced by the GEC ESTRO in 2005 [16] has been thoroughly validated, is reliable and reproducible. However it was primarily described for reporting only. Although there is growing evidence that this target concept is feasible, uncertainties in different aspects around this concept have to be assumed. Furthermore, during the last decade of manual optimisation performed at different institutions [1–3,19], the treatment planning concept has been a more complex approach than the application of a simple set of dose constraints. Each manual treatment plan started systematically with a standard loading pattern, and a pear-shaped isodose normalised to point A. Based on the visual inspection and critical judgement of this dose distribution, adaptations were done. This procedure represented a clinically and dosimetric conservative approach for introducing changes. This was regarded as essential due to the excellent therapeutic ratio which has been clinically reported for cervical cancer brachytherapy so far.

Dwell positions in the cranial part of the tandem were only reduced in the case of sigmoid colon overdosage. Changes in the ring were done if the dose for bladder and/or rectum was critical. The normalisation point was not allowed to be set more than 25 mm perpendicularly from the intrauterine channel. This led to the overall limitation of the dwell times and consequently also to the dose

to normal tissue around the target in regions where no explicit OAR contours had been drawn. The dose resulting from the ring loading was distributed to several positions, with no substantial difference in dwell weight. Larger hot spots around single ring positions were thus avoided. This is not detectable with DVH parameters as applied, but it would affect directly the surface and tissue depth dose in the vagina.

Furthermore, in the case of patients with large HR CTV substantially deviating from the pear shape or with major residual disease at brachytherapy, the use of interstitial needles is an essential part of optimisation in addition to the intracavitary applicator (Vienna ring applicator [20,21]). These needles are considered as tools only to fine-tune the dose distribution, while still most of the dose distribution was based on the intracavitary part. This is a completely different approach compared to the classical concept of interstitial brachytherapy which expects equal dwell times (activity) in each catheter (e.g. the Paris system). The dwell weights for needle positions were therefore limited to 20%, and only in extreme cases up to 30%, compared to the 100% dwell weights used in the tandem and/or the ring.

Dwell time analysis shows that treatment plans optimised with HIPO tend to cover most of the HR CTV with the dose coming from *T*/*R* (Table 4). Dose from interstitial needles is low, even significantly lower than in manually optimised plans. Also the ring loading was decreased, which may become important for improving the future sparing of the vaginal wall. In HIPO, *T*/*R* is optimised first and needles afterwards only to cover the missing parts of the HR CTV. This avoids the occurrence of hot spots as shown and reduces the high-dose regions in the parametrium and the dose to the vagina. If the *T*/*R* and needles were optimised at the same time and with equal weighting, they would have equal importance in the inverse optimisation algorithm. The result would be high loading of needles and thus larger high-dose regions in surrounding normal tissue. There is no clear rationale to use, or even to allow for, such a dosimetric system.

### *Specific features of inverse planning with HIPO*

The first essential tool to take these additional constraints into account as comprehensively as possible is the dwell gradient restriction. This tool was initially introduced for point dose optimisation in the Plato TPS v14.3. Chajon proposed delineating structures around the applicator and involving them in the inverse planning for IPSA to mimic dwell time gradient restriction in gynaecological brachytherapy [5]. Dwell time gradient restriction forces the system to avoid single positions with very high dwell times and dwell time reduction to zero even if the position is not needed to cover the contoured target. This limits first the size of contiguous high-dose regions around single dwell positions in needles and around the *T*/*R*, and second, it forces the optimiser to extend the dose distribution in a direction where the additional loading has been placed outside the HR CTV. The last point is related to the caudal part of the tandem, which should not be set to zero, even if there is no HR CTV. The dwell time gradient restriction is more important for *T*/*R* positions with high dwell times, compared to needle positions used for fine-tuning.

The most important tool used when optimising Vienna ring applications is the toggling between *T*/*R* and needles optimisation. It allows the procedure to be performed in a similar way to the manual optimisation and automatically results in lower dwell times for the needles. In most of the patients, clinically acceptable results were already obtained after the first run of *T*/*R* and needles optimisation. The consecutive iterations, as provided by HIPO, can be used to improve dose distribution even further.

The dosimetric analysis of vagina wall was performed in order to verify if HIPO is able to eliminate big hotspots in surrounding tissues, since vagina is the OAR closest to the applicator. Although anatomical and/or dosimetric assessment of vagina wall is influenced by major uncertainties and therefore no dose–volume parameters are recommended for prospective treatment planning [30], the vaginal wall can be used as a relative parameter to reflect the dose distribution outside of the HR CTV. From Table 5 it is apparent that HIPO is able to spare the vagina wall at least to the same level as manual planning. The mean of all evaluated parameters is even better in favour of HIPO. Parameters such as $D_{0.1cc}$ for *T*/*R* configuration and V200 and $D_{1cc}$ for *T*/*R* + *N* configuration are significantly lower when HIPO is used. It would be practical to have a tool for automatic delineation of vagina wall based on applicator surface that would allow delineation of vagina wall and its integration into the process of inverse planning.

### *Treatment planning time*

Another important aspect of treatment planning is the time required to create a clinically acceptable treatment plan. This issue was not studied in detail as an objective comparison is not yet possible. Manual planning is the state of the art, and the physics authors involved in this analysis have performed more than 100 manual plan optimisations in clinical routine. The experience with inverse planning has been started only recently and inverse planning is now slowly being introduced into clinical practice. Furthermore a scientific analysis would have to be done in more detail with comparison and analysis of each individual step of the planning procedure.

## Conclusion

Inverse planning based on the HIPO algorithm can produce treatment plans for cervical cancer brachytherapy which are comparable to plans based on manual optimisation as applied in clinical practice. The inverse plans, with either *T*/*R* or combined intracavitary/interstitial applicators, following the in-house Vienna planning protocol, currently fulfil all requirements which have been developed and validated within the clinical planning setting. It is essential that the spatial dose distribution in addition to the DVH-based constraints is taken into account. The proposed inverse planning concept is feasible for improving the therapeutic ratio and limiting the substantial high-dose regions around the needles.

## Acknowledgements

We are grateful to Aphiyut Udomphon (Radiation-Oncology, Chiang Mai University, Thailand) for the help with direct reconstruction of the applicator during his fellowship at the Department of Radiotherapy, Medical University of Vienna.

## References

[1] Kirisits C, Potter R, Lang S, et al. Dose and volume parameters for MRI-based treatment planning in intracavitary brachytherapy for cervical cancer. Int J Radiat Oncol Biol Phys 2005;62:901–11.
[2] Lindegaard JC, Tanderup K, Nielsen SK, Haack S, Gelineck J. MRI-guided 3D optimization significantly improves DVH parameters of pulsed-dose-rate brachytherapy in locally advanced cervical cancer. Int J Radiat Oncol Biol Phys 2008;71:756–64.
[3] De Brabandere M, Mousa AG, Nulens A, Swinnen A, Van Limbergen E. Potential of dose optimisation in MRI-based PDR brachytherapy of cervix carcinoma. Radiother Oncol 2008;88:217–26.
[4] Bortfeld T. Optimized planning using physical objectives and constraints. Semin Radiat Oncol 1999;9:20–34.
[5] Chajon E, Dumas I, Touleimat M, et al. Inverse planning approach for 3-D MRI-based pulse-dose rate intracavitary brachytherapy in cervix cancer. Int J Radiat Oncol Biol Phys 2007;69:955–61.
[6] Lessard E, Hsu IC, Pouliot J. Inverse planning for interstitial gynecologic template brachytherapy: truly anatomy-based planning. Int J Radiat Oncol Biol Phys 2002;54:1243–51.

[7] Dewitt KD, Hsu IC, Speight J, et al. 3D inverse treatment planning for the tandem and ovoid applicator in cervical cancer. Int J Radiat Oncol Biol Phys 2005;63:1270–4.
[8] Pouliot J, Lessard É, Hsu I-C. Chapter 21 – advanced 3D planning. In: Brachytherapy physics. M.P. Publishing; 2005. AAPM – ABS. p. 393 – 413.
[9] Karabis A, Giannouli S, Baltas D. HIPO: a hybrid inverse treatment planning optimization algorithm in HDR brachytherapy. Radiother Oncol 2005;76:S29.
[10] Kubicky CD, Yeh BM, Lessard E, et al. Inverse planning simulated annealing for magnetic resonance imaging-based intracavitary high-dose-rate brachytherapy for cervical cancer. Brachytherapy 2008;7:242–7.
[11] Lachance B, Beliveau-Nadeau D, Lessard E, et al. Early clinical experience with anatomy-based inverse planning dose optimization for high-dose-rate boost of the prostate. Int J Radiat Oncol Biol Phys 2002;54:86–100.
[12] Lahanas M, Schreibmann E, Baltas D. Multiobjective inverse planning for intensity modulated radiotherapy with constraint-free gradient-based optimization algorithms. Phys Med Biol 2003;48:2843–71.
[13] Lahanas M, Baltas D, Zamboglou N. A hybrid evolutionary algorithm for multi-objective anatomy-based dose optimization in high-dose-rate brachytherapy. Phys Med Biol 2003;48:399–415.
[14] Milickovic N, Lahanas M, Papagiannopoulo M, Zamboglou N, Baltas D. Multiobjective anatomy-based dose optimization for HDR-brachytherapy with constraint free deterministic algorithms. Phys Med Biol 2002;47:2263–80.
[15] Ehrgott M. Chapter 3: the weighted sum method and related topics. In: Multicriteria optimization. Berlin, Heidelberg: Springer; 2005.
[16] Haie-Meder C, Potter R, Van Limbergen E, et al. Recommendations from gynaecological (GYN) GEC-ESTRO working group (I): concepts and terms in 3D image based 3D treatment planning in cervix cancer brachytherapy with emphasis on MRI assessment of GTV and CTV. Radiother Oncol 2005;74:235–45.
[17] Potter R, Haie-Meder C, Van Limbergen E, et al. Recommendations from gynaecological (GYN) GEC ESTRO working group (II): concepts and terms in 3D image-based treatment planning in cervix cancer brachytherapy-3D dose–volume parameters and aspects of 3D image-based anatomy, radiation physics, radiobiology. Radiother Oncol 2006;78:67–77.
[18] Gerbaulet A, Pötter R, Mazeron J-J, Meertens H, Van Limbergen E. The GEC ESTRO handbook of brachytherapy. ESTRO; 2002.
[19] Chargari C, Magne N, Dumas I, et al. Physics contributions and clinical outcome with 3D-MRI-based pulsed-dose-rate intracavitary brachytherapy in cervical cancer patients. Int J Radiat Oncol Biol Phys. 2009;74:133–9.
[20] Dimopoulos JC, Kirisits C, Petric P, et al. The Vienna applicator for combined intracavitary and interstitial brachytherapy of cervical cancer: clinical feasibility and preliminary results. Int J Radiat Oncol Biol Phys 2006;66:83–90.
[21] Kirisits C, Lang S, Dimopoulos J, et al. The Vienna applicator for combined intracavitary and interstitial brachytherapy of cervical cancer: design, application, treatment planning, and dosimetric results. Int J Radiat Oncol Biol Phys 2006;65:624–30.
[22] Potter R, Dimopoulos J, Georg P, et al. Clinical impact of MRI assisted dose–volume adaptation and dose escalation in brachytherapy of locally advanced cervix cancer. Radiother Oncol 2007;83:148–55.
[23] Berger D, Dimopoulos J, Potter R, Kirisits C. Direct reconstruction of the Vienna applicator on MRI images. Radiother Oncol 2009;93:347–51.
[24] Lang S, Kirisits C, Dimopoulos J, Georg D, Potter R. Treatment planning for MRI assisted brachytherapy of gynecologic malignancies based on total dose constraints. Int J Radiat Oncol Biol Phys 2007;69:619–27.
[25] Kirisits C, Trnkova P, Baltas D, Dimopoulos J, Potter R. Inverse optimization for cervix cancer brachytherapy including automatic loading, DVH optimization and modification restriction adapted from manual planning. Med Phys 2008;35:2726.
[26] Potter R, Knocke TH, Fellner C, et al. Definitive radiotherapy based on HDR brachytherapy with iridium 192 in uterine cervix carcinoma: report on the Vienna University Hospital findings (1993–1997) compared to the preceding period in the context of ICRU 38 recommendations. Cancer Radiother 2000;4:159–72.
[27] Fellner C, Potter R, Knocke TH, Wambersie A. Comparison of radiography- and computed tomography-based treatment planning in cervix cancer in brachytherapy with specific attention to some quality assurance aspects. Radiother Oncol 2001;58:53–62.
[28] Viswanathan AN, Erickson B. 3D Image-guided gynecologic brachytherapy: practice patterns in the United States. Brachytherapy 2008;7:110.
[29] Gerbaulet A, Michel G, Haie-Meder C, et al. The role of low dose rate brachytherapy in the treatment of cervix carcinoma. Experience of the Gustave-Roussy Institute on 1245 patients. Eur J Gynaecol Oncol 1995;16:461–75.
[30] Berger D, Dimopoulos J, Georg P, et al. Uncertainties in assessment of the vaginal dose for intracavitary brachytherapy of cervical cancer using a tandem-ring applicator. Int J Radiat Oncol Biol Phys 2007;67:1451–9.